Supplementary Information

Insight into Effects of Crystal Phase of Ru over Ultrathin Ru@Pt Core-Shell Nanosheets for Methanol Electrooxidation

Junjun Li,† Man Hou,† and Zhicheng Zhang*

Department of Chemistry, School of Science, Tianjin University & Tianjin Key Laboratory of Molecular Optoelectronic Sciences, Tianjin 300072, China

*Correspondence to: zczhang19@tju.edu.cn

Experimental Section

Materials. Ruthenium (III) chloride hydrate ($RuCl_3 \cdot xH_2O$, 99.98%), poly-(vinylpyrrolidone) (PVP, MW = 29000), glycine (99%), formaldehyde solution (HCHO, 37%) and other chemicals used in the experiments without special mention were all purchased from Sigma-Aldrich. Potassium tetrachloroplatinate(II) (K_2PtCl_4, 99.9%) was purchased from Alfa Aesar. Ethanol (absolute, 99.9%) and acetone (99.9%) were purchased from Merck (Nordic European Centre, Singapore). All the chemicals were used as received without further purification. Milli-Q water with resistivity of 18.2 MΩ·cm was obtained through the Milli-Q system.

Synthesis of Ru_{fcc} nanosheets (NSs). The ultrathin Ru_{fcc} NSs were synthesized by using a modified protocol based on a previous report.[1] Briefly, after the PVP (100.0 mg) and $RuCl_3 \cdot xH_2O$ (12.5 mg) were dissolved in water (10 mL), HCHO (37 wt%, 0.4 mL) and water (4.6 mL) were successively added into the aforementioned solution and magnetically stirred for 15 min. The resulting homogeneous dark solution was transferred into a 23 mL Teflon-lined stainless steel autoclave which was maintained at 160 ^{o}C for 4 h and then cooled down to room temperature naturally. Finally, the resulting product was collected by centrifugation at 12,000 rpm for 10 min, and further purified three times by a mixture of ethanol (10 mL) and acetone (30 mL).

Synthesis of Ru_{hcp} NSs. The ultrathin Ru_{hcp} NSs were synthesized by using a modified protocol based on a previous report.[1] Briefly, after PVP (200.0 mg) and $RuCl_3 \cdot xH_2O$ (93.4 mg) were dissolved in water (10 mL), HCHO (37 wt%, 0.4 mL) and water (4.6 mL) were successively added into the aforementioned solution and magnetically stirred for 15 min. The resulting homogeneous dark solution was transferred into a 23 mL Teflon-lined stainless steel autoclave which was maintained at 160 ^{o}C for 8 h and then cooled down to room temperature naturally. Finally, the resulting product was collected by centrifugation at 12,000 rpm for 10 min, and further purified three times by a mixture of ethanol (10 mL) and acetone (30 mL).

Synthesis of Ru_{fcc}@Pt NSs. In a typical procedure for the synthesis of Ru_{fcc}@Pt NSs, PVP (50.0 mg), glycine (75.0 mg) and K_2PtCl_4 (0.8 mg) were first dissolved in water (7.5 mL), and then mixed with the suspension of the aforementioned Ru_{fcc} NSs in water (0.524 mg/mL, 0.5 mL) under vigorous stirring. The resulting mixture was transferred into a 23 mL Teflon-lined stainless steel autoclave which was maintained at 160 ^{o}C for 8 h and then cooled down to room temperature naturally. Finally, the resulting product was collected by centrifugation at 12,000 rpm for 10 min, and washed three times with water and three times with ethanol.

Synthesis of Ru_{hcp}@Pt NSs. In a typical procedure for the synthesis of Ru_{hcp}@Pt NSs, PVP (50.0 mg), glycine (75.0 mg) and K_2PtCl_4 (2.4 mg) were first dissolved in water (7.5 mL), and then mixed with the suspension of the aforementioned Ru_{hcp} NSs in water (0.661 mg/mL, 0.5 mL) under vigorous stirring. The resulting mixture was transferred into a 23 mL Teflon-lined stainless steel autoclave which was maintained at 180 ^{o}C for 8 h and then cooled down to room temperature naturally. Finally, the resulting product was collected by centrifugation at 12,000 rpm for 10 min, and washed three times with water and three times with ethanol.

Electrochemical measurements. The electrochemical methanol oxidation reaction (MOR) was conducted by cyclic voltammetry (CV) at scan rate of 50 mV/s in N_2-saturated 0.5 M H_2SO_4 aqueous solution containing 1 M methanol on a CHI-760E (CH Instruments, Inc.). The catalyst modified glassy carbon electrode (GCE, 3 mm in diameter), Ag/AgCl electrode, and Pt wire were used as the working, reference, and counter electrodes, respectively. The preparation of working electrode is shown as follows. First, a GCE was polished with 300 and 50 nm Al_2O_3 powders successively, and then washed with ethanol and water, respectively. After drying in air, 3.1 μL of Ru_{fcc}@Pt NSs dispersion in ethanol (ca. 0.644 mg_{Pt}/mL) or 4.1 μL of Ru_{hcp}@Pt NSs (ca. 0.489 mg_{Pt}/mL) was dropped onto its surface and dried in air for 0.5 h. The as-prepared Ru_{fcc}@Pt NSs-coated GCE was irradiated with a UV lamp (10 W with emission of 185 and 254 nm), which was placed about 5 mm away from the GCE, for 4 h to remove the capping agent on Ru_{fcc}@Pt NSs.[2-4] Finally, 1.5 μL of 0.5 wt% Nafion ethanolic solution was dropped onto the surface of Ru_{fcc}@Pt NSs-coated GCE and dried in air for 1 h. The modified electrode was used as the working electrode for the MOR.

The preparation of commercial Pt/C modified GCE was based on the aforementioned method. Briefly, 15 mg of commercial Pt/C (20 wt% of Pt nanoparticles supported on carbon black, Alfar Aesar, America) was mixed with 10 mL of the mixture of ethanol and water (v:v=1:1) to form the Pt/C dispersion (1.5 mg/mL). Then 3.4 μL of the prepared Pt/C dispersion was dropped onto the surface of pre-treated RDE as mentioned above and dried in air for 2 h. Finally, 1.5 μL of 0.5 wt% Nafion ethanolic solution was dropped onto the surface of commercial Pt/C-coated GCE and dried in air for 1 h. The modified electrode was used as the working electrode for the MOR.

Characterization. Samples for transmission electron microscopy (TEM) analyses were prepared by dropping the nanocrystal ethanolic dispersion on holey carbon-coated copper grids and then dried under ambient conditions. The low-magnification TEM images were taken on a JEOL JEM-2100F operated at 200 kV. The high-angle annular dark-field scanning transmission electron microscope (HAADF-STEM) and energy-dispersive X-ray spectroscopy (EDS) elemental mapping and line scanning profiles were recorded on a high resolution aberration corrected transmission electron microscope JEOL JEM-ARM200F operated at 200 kV. Samples for X-ray photoelectron spectroscopy (XPS) were prepared by dropping the nanocrystal ethanolic dispersion on a piranha-cleaned Si and then dried under ambient conditions. The XPS data were collected with a Theta Probe electron spectrometer (ESCA-Lab-200i-XL, Thermo Scientific). The energy calibration was made against the C1s peak during analysis. Inductively coupled plasma optical emission spectrometry (ICP-OES) was performed on a Dual-view Optima 5300 DV ICP-OES system.

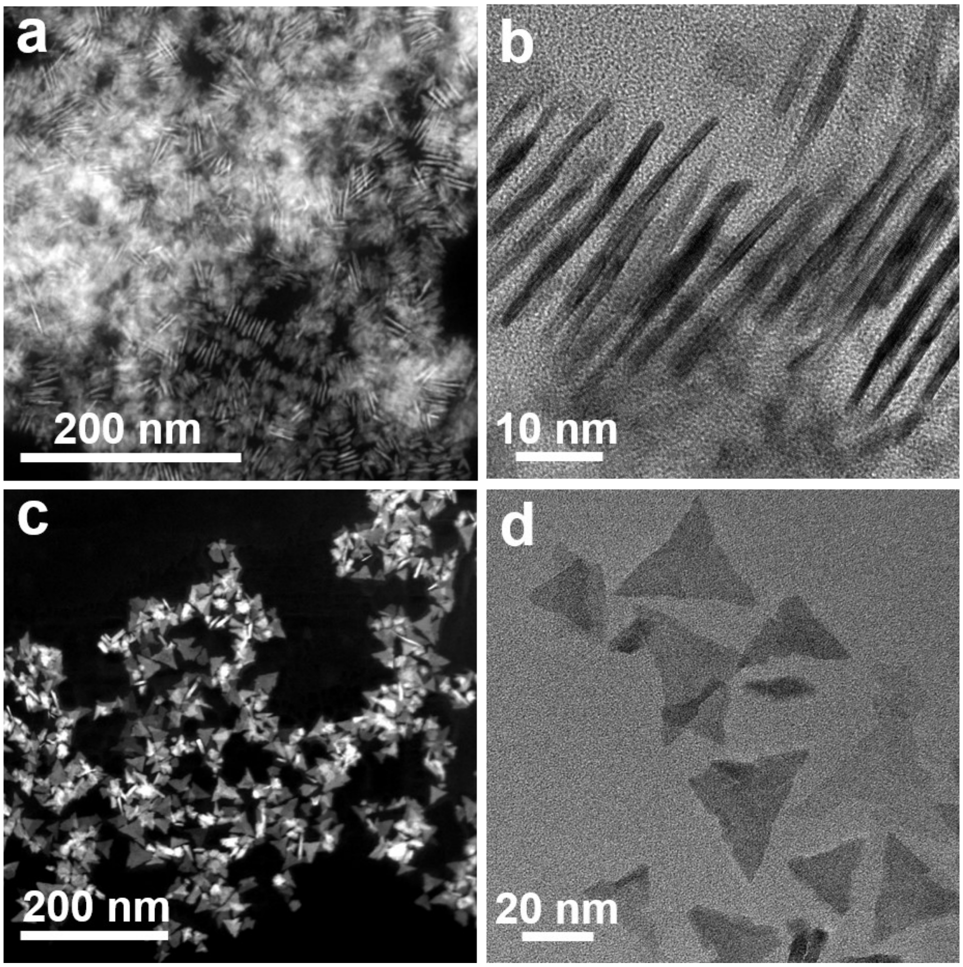

Figure S1. (a) HAADF-STEM and (b) TEM images of Ru_{hcp} NSs. (c) HAADF-STEM and (d) TEM images of Ru_{fcc} NSs.

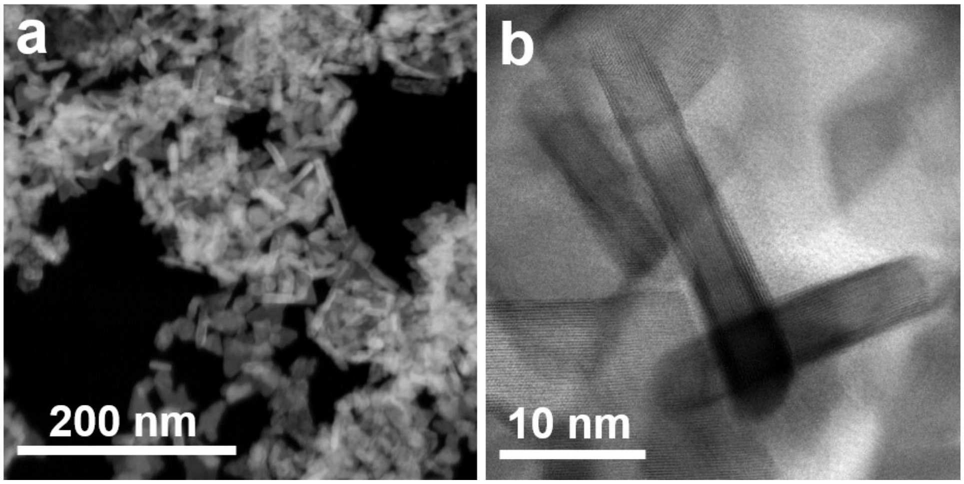

Figure S2. (a) HAADF-STEM and (b) TEM images of Ru_{fcc}@Pt NSs.

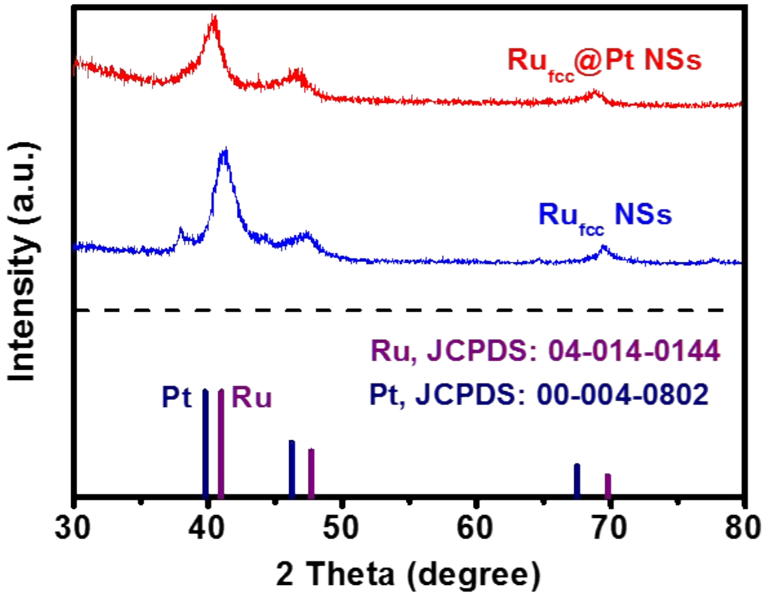

Figure S3. XRD pattern of Ru_{fcc}@Pt NSs.

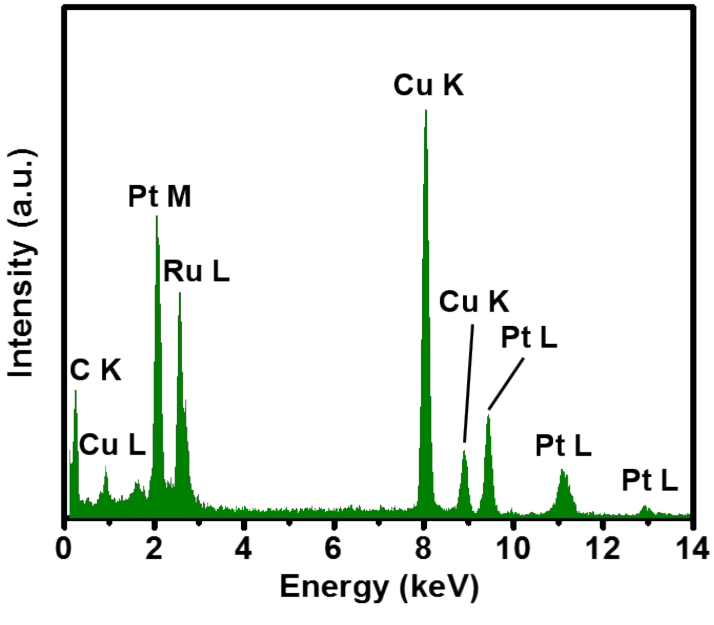

Figure S4. A representative EDS spectrum of Ru_{fcc}@Pt NSs, showing that the atomic ratio of Pt to Ru is 40.5/59.5. The additional Cu signal arises from the copper TEM grid.

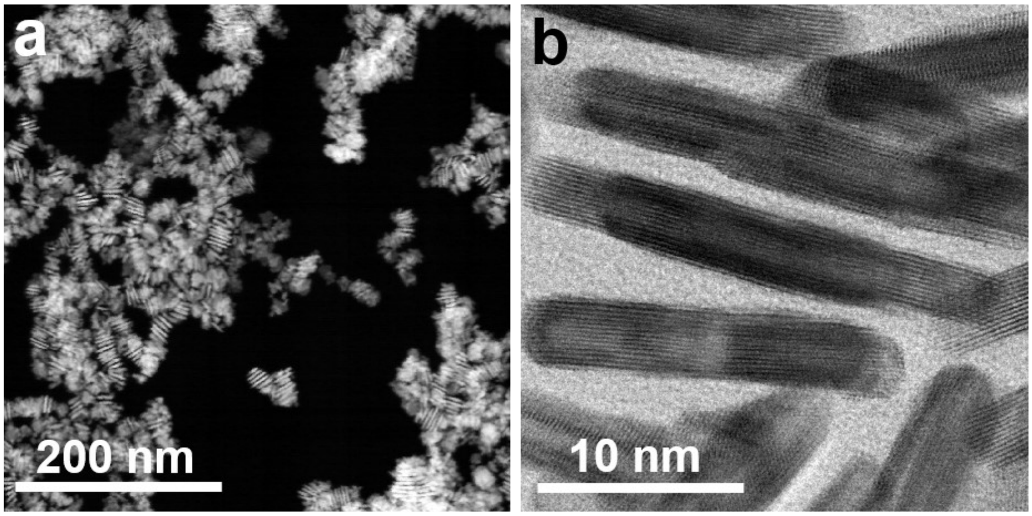

Figure S5. (a) HAADF-STEM and (b) BF-STEM images of Ru_{hcp}@Pt NSs.

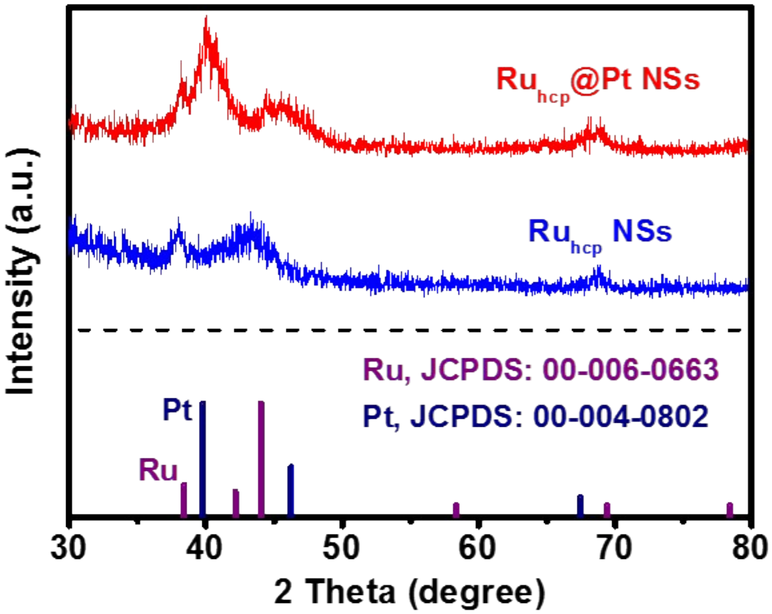

Figure S6. XRD pattern of Ru_{hcp}@Pt NSs.

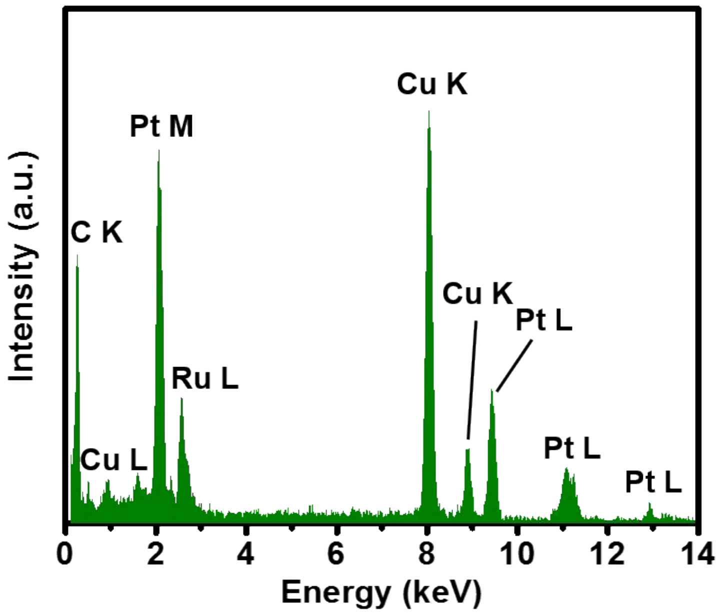

Figure S7. A representative EDS spectrum of Ru_{hcp}@Pt NSs, showing that the atomic ratio of Pt to Ru is 64.1/35.9. The additional Cu signal arises from the copper TEM grid.

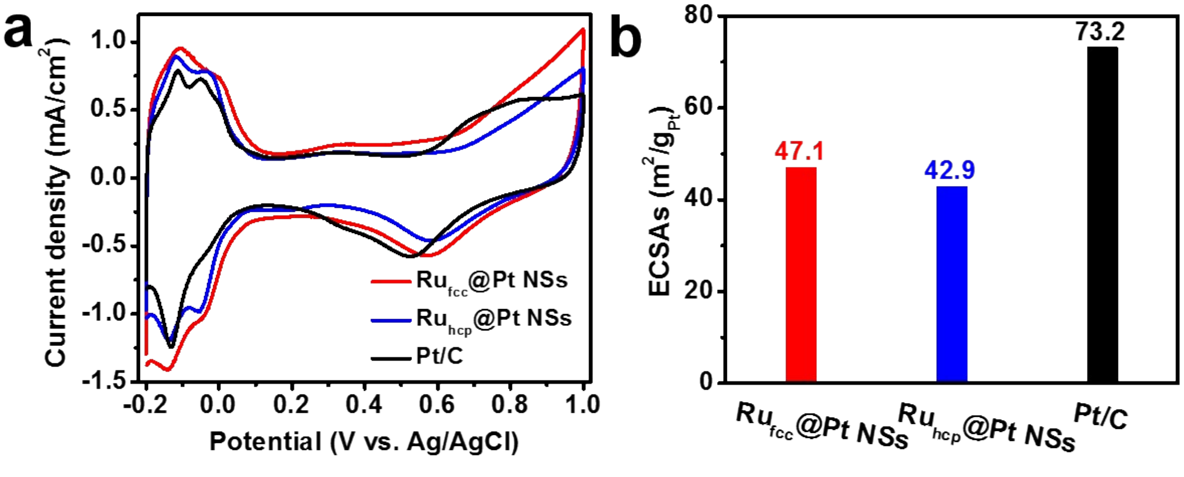

Figure S8. (a) CV curves of Ru_{fcc}@Pt NSs, Ru_{hcp}@Pt NSs and commercial Pt/C catalyst in N_2-saturated 0.5 M H_2SO_4 aqueous solution at scan rate of 50 mV/s. (b) The ECSAs of Ru_{fcc}@Pt NSs, Ru_{hcp}@Pt NSs and commercial Pt/C catalyst.

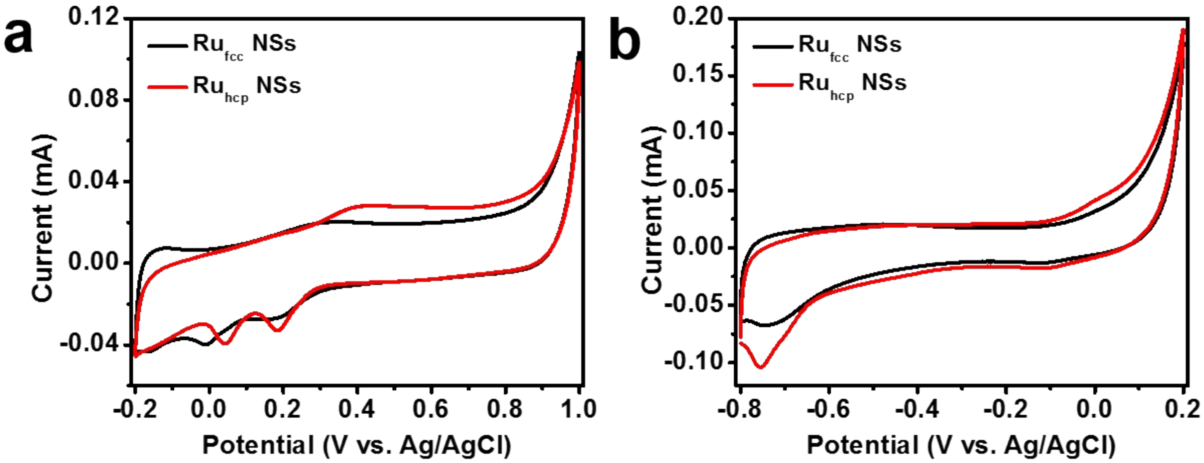

Figure S9. CV curves of Ru$_{fcc}$ NSs and Ru$_{hcp}$ NSs in (a) 0.5 M H_2SO_4 aqueous solution containing 1 M methanol and (b) 1 M KOH aqueous solution containing 1 M methanol at scan rate of 50 mV/s.

Table S1. Comparison of electrocatalytic performance of various Pt-based catalysts toward MOR under acidic condition.

Sample	Specific activity (mA/cm^2)	Mass activity (A/mg_{Pt})	Electrolyte	Reference
Ru_{fcc}@Pt NSs	1.13	0.530	0.5 M H_2SO_4 + 1 M methanol	This work
Ru_{hcp}@Pt NSs	0.910	0.391	0.5 M H_2SO_4 + 1 M methanol	This work
Pt/C	0.513	0.375	0.5 M H_2SO_4 + 1 M methanol	This work
PtZn/MWNT	1.08	0.612	0.5 M H_2SO_4 + 1 M methanol	5
Pt/imidazolium salt-ionic liquid/CNT	0.606	0.410	0.5 M H_2SO_4 + 0.5 M methanol	6
Spherical Pt-Zn nanocrystals	0.980	0.190	0.1 M H_2SO_4 + 0.5 M methanol	7
Ultrathin Pt NWs	~1.1	~0.500	0.5 M H_2SO_4 + 0.5 M methanol	8
Pt/N-doped graphene	-	~0.400	0.5 M H_2SO_4 + 1 M methanol	9
Pt/N-doped porous carbon	1.39	0.343	0.5 M H_2SO_4 + 1 M methanol	10
PtRu/HPMo-CS-CNTs	0.316	0.232	0.5 M H_2SO_4 + 1 M methanol	11
Pt_3Ti/C	0.307	0.149	0.1 M $HClO_4$ + 1 M methanol	12

Pt_3V/C	0.384	0.200	0.1 M $HClO_4$ + 1 M methanol	12
Pt CNCs	1.190	0.118	0.5 M H_2SO_4 + 2 M methanol	13
Pt/graphene and g-C_3N_4 hybrids	15.7	0.613	1 M H_2SO_4 + 2 M methanol	14
Pt-on-Pd nanodendrites	-	0.49	0.5 M H_2SO_4 + 1 M methanol	15
Spherical Pt_3Zn intermetallic NCs	~0.93	~0.26	0.1 M H_2SO_4 + 0.5 M methanol	16
Cubic Pt-Zn alloy NCs	~0.73	~0.19	0.1 M H_2SO_4 + 0.5 M methanol	16
Pt_3Co NWs/C	1.95	1.02	0.1 M $HClO_4$ + 0.2 M methanol	17
PtPb/Pt core/shell nanoplate	2.7	1.5	0.1 M $HClO_4$ + 0.1 M methanol	18
Pt-CeO_2-rods	2.04	-	0.5 M H_2SO_4 + 1 M methanol	19

MWNT: multiwalled carbon nanotube; NSs: nanosheets; CNTs: carbon nanotubes; NCs: nanocrystals; NWs: nanowires; HPMo-CS-CNTs: heteropolyacid of phosphomolybdic acid (HPMo) and chitosan (CS) functionalized CNTs; CNCs: concave nanocubes.

Table S2. Comparison of electrocatalytic performance of various Pt-based catalysts toward MOR under basic condition.

Sample	Specific activity (mA/cm^2)	Mass activity (A/mg$_{Pt}$)	Electrolyte	Reference
Ru$_{fcc}$@Pt$_{fcc}$ NSs	3.48	1.64	1 M KOH + 1 M methanol	This work
Ru$_{hcp}$@Pt$_{fcc}$ NSs	2.96	1.27	1 M KOH + 1 M methanol	This work
Pt/C	1.63	1.19	1 M KOH + 1 M methanol	This work
PtZn/MWNT	~1.14	~0.542	0.1 M KOH + 0.5 M methanol	5
Pt$_{0.5}$Ag/C	-	2.92	0.5 M KOH + 2 M methanol	20
Pt/Ni(OH)$_2$/rGO Ternary hybrids	150	1.07	1 M KOH + 1 M methanol	21
Pt-rich shell coated Ni NPs	-	0.290	1 M KOH + 1 M methanol	22
PtAu-rGO	0.84	0.637	1 M KOH + 1 M methanol	23
PtNi/C	-	1.20	1 M KOH + 1 M methanol	24
Pt nanoflowers-TiO$_2$ arrays-rGO	4.40	-	0.5 M KOH + 1 M methanol	25
Pt-TiO$_2$/ITO	1.80	-	1 M KOH + 1 M methanol	26
Porous Pt NTs	~5.00	2.33	1 M KOH + 1 M methanol	27
Macroporous Pt NTs	0.393	1.13	1 M KOH + 1 M methanol	27

GrPt	-	0.939	1 M NaOH + 1 M methanol	28

rGO: reduced graphene oxide; NPs: nanoparticles; ITO: indium tin oxide; NTs: nanotubes.

References

[1] A.-X. Yin, W.-C. Liu, J. Ke, W. Zhu, J. Gu, Y.-W. Zhang, C.-H. Yan, *J. Am. Chem. Soc.* **2012**, *134*, 20479.

[2] C. Aliaga, J. Y. Park, Y. Yamada, H. S. Lee, C. K. Tsung, P. Yang, G. A. Somorjai, *J. Phys. Chem. C* **2009**, *113*, 6150.

[3] M. Crespo-Quesada, J.-M. Andanson, A. Yarulin, B. Lim, Y. Xia, L. Kiwi-Minsker, *Langmuir* **2011**, *27*, 7909.

[4] C. Wang, H. Daimon, Y. Lee, J. Kim, S. Sun, *J. Am. Chem. Soc.* **2007**, *129*, 6974.

[5] Z. Qi, C. Xiao, C. Liu, T. W. Goh, L. Zhou, R. Maligal-Ganesh, Y. Pei, X. Li, L. A. Curtiss, W. Huang, *J. Am. Chem. Soc.* **2017**, *139*, 4762.

[6] S. Guo, S. Dong, E. Wang, *Adv. Mater.* **2010**, *22*, 1269.

[7] Y. Kang, J. B. Pyo, X. Ye, T. R. Gordon, C. B. Murray, *ACS Nano* **2012**, *6*, 5642.

[8] B. Y. Xia, H. B. Wu, Y. Yan, X. W. Lou, X. Wang, *J. Am. Chem. Soc.* **2013**, *135*, 9480.

[9] B. Xiong, Y. Zhou, Y. Zhao, J. Wang, X. Chen, R. O'Hayre, Z. Shao, *Carbon* **2013**, *52*, 181.

[10] F. Su, Z. Tian, C. K. Poh, Z. Wang, S. H. Lim, Z. Liu, J. Lin, *Chem. Mater.* **2010**, *22*, 832.

[11] Z. Cui, C. M. Li, S. P. Jiang, *Phys. Chem. Chem. Phys.* **2011**, *13*, 16349.

[12] Z. Cui, H. Chen, M. Zhao, D. Marshall, Y. Yu, H. Abruna, F. J. DiSalvo, *J. Am. Chem. Soc.* **2014**, *136*, 10206.

[13] Z.-C. Zhang, J.-F. Hui, Z.C. Liu, X. Zhang, J. Zhuang, X. Wang, *Langmuir* **2012**, *28*, 14845.

[14] H. Huang, S. Yang, R. Vajtai, X. Wang, P. M. Ajayan, *Adv. Mater.* **2014**, *26*, 5160.

[15] L. Wang, Y. Nemoto, Y. Yamauchi, *J. Am. Chem. Soc.* **2011**, *133*, 9674.

[16] Y. Kang, J. B. Pyo, X. Ye, T. R. Gordon, C. B. Murray, *ACS Nano* **2012**, *6*, 5642.

[17] L. Bu, S. Guo, X. Zhang, X. Shen, D. Su, G. Lu, X. Zhu, J. Yao, J. Guo, X. Huang, *Nat. Commun.* **2016**, *7*, 11850.

[18] L. Bu, N. Zhang, S. Guo, X. Zhang, J. Li, J. Yao, T. Wu, G. Lu, J.-Y. Ma, D. Su, X. Huang, *Science* **2016**, *354*, 1410.

[19] W. Chen, J. Xue, Y. Bao, L. Feng, *Chem. Eng. J.* **2020**, *381*, 122752.

[20] Y.-Y. Feng, L.-X. Bi, Z.-H. Liu, D.-S. Kong, Z.-Y. Yu, *J. Catal.* **2012**, *290*, 18.

[21] W. Huang, H. Wang, J. Zhou, J. Wang, P. N. Duchesne, D. Muir, P. Zhang, N. Han, F. Zhao, M. Zeng, J. Zhong, C. Jin, Y. Li, S.-T. Lee, H. Dai, *Nat. Commun.* **2015**, *6*, 10035.

[22] X.-Z. Fu, Y. Liang, S.-P. Chen, J.-D. Lin, D.-W. Liao, *Catal. Commun.* **2009**, *10*, 1893.

[23] J.-N. Zheng, S.-S. Li, X. Ma, F.-Y. Chen, A.-J. Wang, J.-R. Chen, J.-J. Feng, *J. Mater. Chem. A.* **2014**, *2*, 8386.

[24] Q. Jiang, L. Jiang, S. Wang, J. Qi, G. Sun, *Catal. Commun.* **2010**, *12*, 67.

[25] C. Zhai, M. Zhu, D. Bin, H. Wang, Y. Du, C. Wang, P. Yang, *ACS Appl. Mater. Interfaces* **2014**, *6*, 17753.

[26] H. Zhang, W. Zhou, Y. Du, P. Yang, C. Wang, J. Xu, *J. Hydrogen Energy* **2010**, *35*, 13290.

[27] Y. Lou, C. Li, X. Gao, T. Bai, C. Chen, H. Huang, C. Liang, Z. Shi, S. Feng, *ACS Appl. Mater. Interfaces* **2016**, *8*, 16147.

[28] C. Berghian-Grosan, T. Radu, A. R. Biris, M. Dan, C. Voica, F. Watanabe, A. S. Biris, A. Vulcu, *J. Energy Chem.* **2020**, *40*, 81.